

An Integrated Neuro-mechanical Model of *C. elegans* Forward Locomotion

Jordan H. Boyle, John Bryden and Netta Cohen

School of Computing, University of Leeds, Leeds LS2 9JT, United Kingdom

Abstract. One of the most tractable organisms for the study of nervous systems is the nematode *Caenorhabditis elegans*, whose locomotion in particular has been the subject of a number of models. In this paper we present a first integrated neuro-mechanical model of forward locomotion. We find that a previous neural model is robust to the addition of a body with mechanical properties, and that the integrated model produces oscillations with a more realistic frequency and waveform than the neural model alone. We conclude that the body and environment are likely to be important components of the worm's locomotion subsystem.

1 Introduction

The ultimate aim of neuroscience is to unravel and completely understand the links between animal behaviour, its neural control and the underlying molecular and genetic computation at the cellular and sub-cellular levels. This daunting challenge sets a distant goal post in the study of the vast majority of animals, but work on one animal in particular, the nematode *Caenorhabditis elegans*, is leading the way. This tiny worm has only 302 neurons and yet is capable of generating an impressive wealth of sensory-motor behaviours. With the first fully sequenced animal genome [1], a nearly complete wiring diagram of the nervous circuit [2], and hundreds of well characterised mutant strains, the link between genetics and behaviour never seemed more tractable.

To date, a number of models have been constructed of subcircuits within the *C. elegans* nervous system, including sensory circuits for thermotaxis and chemotaxis [3, 4], reflex control such as tap withdrawal [5], reversals (from forward to backward motion and vice versa) [6] and head swing motion [7]. Locomotion, like the overwhelming majority of known motor activity in animals, relies on the rhythmic contraction of muscles, which are controlled or regulated by neural networks. This system consists of a circuit in the head (generally postulated to initiate motion and determine direction) and an additional subcircuit along the ventral cord (responsible for propagating and sustaining undulations, and potentially generating them as well). Models of *C. elegans* locomotion have tended to focus on forward locomotion, and in particular, on the ability of the worm to generate and propagate undulations down its length [8–12]. These models have tended to study either the mechanics of locomotion [8] or the forward locomotion neural circuit [9–12]. In this paper we present simulations of an integrated model of the neural control of forward locomotion [12] with a minimal model

of muscle actuation and a mechanical model of a body, embedded in a minimal environment. The main questions we address are (i) whether the disembodied neural model is robust to the addition of a body with mechanical properties; and (ii) how the addition of mechanical properties alters the output from the motor neurons. In particular, models of the isolated neural circuit for locomotion suffer from a common limitation: the inability to reproduce undulations with frequencies that match the observed behaviour of the crawling worm. To address this question, we have limited our integrated model to a short section of the worm, rather than modelling the entire body. We find that the addition of a mechanical framework to the neural control model of Ref. [12] leads to robust oscillations, with significantly smoother waveforms and reduced oscillation frequencies, matching observations of the worm.

2 Background

2.1 *C. elegans* Locomotion

Forwards locomotion is achieved by propagating sinusoidal undulations along the body from head to tail. When moving on a firm substrate (e.g. agarose) the worm lies on its side, with the ventral and dorsal muscles at any longitudinal level contracting in anti-phase. With the exception of the head and neck, the worm is only capable of bending in the dorso-ventral plane.

Like all nematode worms, *C. elegans* lacks any form of rigid skeleton. Its roughly cylindrical body has a diameter of $\sim 80 \mu\text{m}$ and a length of $\sim 1 \text{ mm}$. It has an elastic cuticle containing (along with its intestine and gonad) pressurised fluid, which maintains the body shape while remaining flexible. This structure is referred to as a hydrostatic skeleton. The body wall muscles responsible for locomotion are anchored to the inside of the cuticle.

2.2 The Neural Model

The neural model used here is based on the work of Bryden and Cohen [11–13]. Specifically, we use the model (equations and parameters) presented in [12] which is itself an extension of Refs. [11, 13]. The model simplifies the neuronal wiring diagram of the worm [2, 14] into a minimal neural circuit for forward locomotion. This reduced model contains a set of repeating *units*, (one “tail” and ten “body” units) where each unit consists of one dorsal motor neuron (of class DB) and one ventral motor neuron (of class VB). A single command interneuron (representing a pair of interneurons of class AVB in the biological worm) provides the “on” signal to the forward locomotion circuit and is electrically coupled (via gap junctions) to all motor neurons of classes DB and VB. In the model, motor neurons also have sensory function, integrating inputs from stretch-receptors, or mechano-sensitive ion channels, that encode each unit’s bending angle. Motor neurons receive both local and – with the exception of the tail – proximate sensory input, with proximate input received from the adjacent posterior unit. The sensory-motor loop for each unit gives rise to local oscillations which phase

lock with adjacent units. Equations and parameters for the neural model are set out in Appendix A.

This neural-only model uses a minimal physical framework to translate neuronal output to bending. Fig. 1B shows the neural model with only two units (a tail and one body unit), as modelled in this paper. In the following section, we outline a more realistic physical model of the body of the worm.

3 Physical Model

Our physical model is an adaptation of Ref. [8], a 2-D model consisting of two rows of N points (representing the dorsal and ventral sides of the worm). Each point is acted on by the opposing forces of the elastic cuticle and pressure, as well as muscle force and drag (often loosely referred to as friction or surface friction [8]). We modify this model by introducing simplifications to reduce simulation time, in part by allowing us to use a longer time step. Fig. 1A illustrates the model’s structure. The worm is represented by a number rigid beams, connected to each of the adjacent beams by four springs. Two horizontal (h) springs connect points on the same side of adjacent beams and resist both elongation and compression. Two diagonal (d) springs connect the dorsal side of the i^{th} beam to the ventral side of the $i + 1^{st}$, and vice versa. These springs strongly resist compression and have an effect analogous to that of pressure, in that they help to maintain reasonably constant area in each unit.

The model was implemented in C++, using a 4th order Runge-Kutta method for numerical integration, with a time step of 0.1 ms.¹ Equations and parameters of the physical model are given in Appendix B. The steps taken to interface the physical and neuronal models are described in Appendix C.

4 Results

Using our integrated model we first simulated a single unit (the tail), and then implemented two phase-lagged units (adding a body unit). In what follows, we present these results, as compared to those of the neural model alone.

4.1 Single Oscillating Segment

The neural model alone produces robust oscillations in unit bending angle (θ_i) with a roughly square waveform, as shown in Fig. 2A. The model unit oscillates at about 3.5 Hz, as compared to frequencies of about 0.5 Hz observed for *C. elegans* forward locomotion on an agarose substrate. It has not been possible to find parameters within reasonable electrophysiological bounds for the neural model that would slow the oscillations to the desired time scales [12].

Oscillations of the integrated neuro-mechanical model of a single unit are shown in Fig. 2B. All but four parameters of the neuronal model remain unchanged from Ref. [12]. However, parameters used for the actuation step caused

¹ The original model [8] required a time step of 0.001 ms with the same integration method.

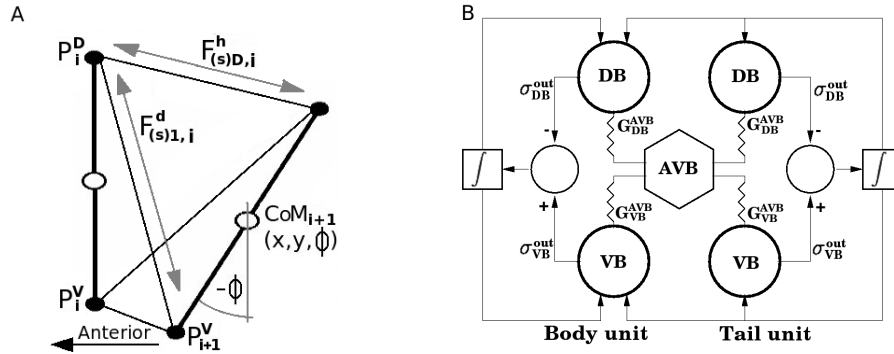


Fig. 1. A: Schematic diagram of the physical model illustrating nomenclature (see Appendix B for details). B: The neural model, with only two units (one body, one tail). AVB is electrically coupled to each of the motor neurons via gap junctions (resistor symbols).

a slight asymmetry in the oscillations when integrated with a physical model, and were therefore modified.

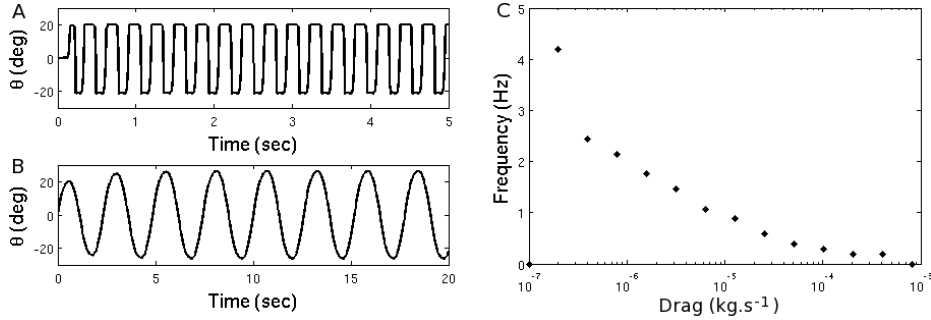


Fig. 2. Oscillations of, A, the original neural model [12] and, B, the integrated model (with drag of $80 \times 10^{-6} kg \cdot s^{-1}$). Note the different time scales. C: Oscillation frequency as a function of drag. The zero frequency point indicates that the unit can no longer oscillate.

As can be seen from the traces in the figure, the frequency of oscillation in the integrated model is about 0.5 Hz for typical agarose drag [8], and the waveform has a smooth, almost sinusoidal shape. Faster (and slower) oscillations are possible for lower (higher) values of drag. Fig. 2C shows a plot of oscillation frequencies as a function of drag for the integrated model.

4.2 Two Phase-lagged Segments

Parameters of the neural model are given in Table A-1 for the tail unit and in Table A-2 for the body unit. Fig. 3 compares bending waveforms recorded from

a living worm (Fig. 3A), simulated by the neural model (Fig. 3B) and simulated by the integrated model (Fig. 3C).

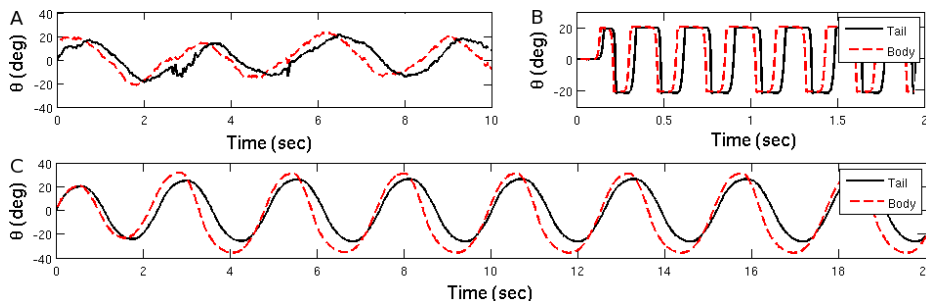


Fig. 3. Phase lagged oscillation of two units. A: Bending angles extracted from a recording of a forward locomoting worm on an agarose substrate. The traces are of two points along the worm (near the middle and $\frac{1}{12}$ of a body length apart). B: Simulation of two coupled units in the neural model. C: Simulation of the integrated model. Take note of the faster oscillations in subplot B.

5 Discussion

C. elegans is amenable to manipulations at the genetic, molecular and neuronal levels but with such rich behaviour being produced by a system with so few components, it can often be difficult to determine the pathways of cause and effect. Mathematical and simulation models of the locomotion therefore provide an essential contribution to the understanding of *C. elegans* neurobiology and motor control.

The inclusion of a realistic embodiment is particularly relevant to a model of *C. elegans* locomotion. Sensory feedback is important to the locomotion of all animals. However, in *C. elegans*, the postulated existence of stretch receptor inputs along the body (unpublished communication, L. Eberly and R. Russel, reported in [2]) would provide direct information about body posture to the motor neurons themselves. Thus, the neural control is likely to be tightly coupled to the shape the worm takes as it locomotes. Modelling the body physics is therefore particularly important in this organism. Here we have presented the first steps in the implementation of such an integrated model, using biologically plausible parameters for both the neural and mechanical components.

One interesting effect is the smoothing of the waveform from a square-like waveform in the isolated neural model to a nearly sinusoidal waveform in the integrated model. The smoothing can be attributed to the body's resistance to bending (modelled as a set of springs), which increases with the bending angle. By contrast, in the original neural model, the rate of bending depends only on the neural output.

The work presented here would naturally lead to an integrated neuro-mechanical model of locomotion for an entire worm. The next step toward this goal, extend-

ing the neural circuit to the entire ventral cord (and the corresponding motor system) is currently underway. The physical model introduces long range interactions between units via the body and environment. In a real worm, as in the physical model, for bending to occur at some point along the worm, local muscles must contract. However, such contractions also apply physical forces to adjacent units, and so on up and down the worm, giving rise to a significant persistence length. For this reason the extension of the neuro-mechanical model from two to three (or more) units will not be automatic and will require parameter changes to model an operable balance between the effects of the muscle and body properties. In fact, the worm’s physical properties (and, in particular, the existence of long range physical interactions along it) could set new constraints on the neural model, or could even be exploited by the worm to achieve more effective locomotion. Either way, the physics of the worm’s locomotion is likely to offer important insights that could not be gleaned from a model of the isolated neural subcircuit.

We have shown that a neural model developed with only the most rudimentary physical framework can continue to function with a more realistic embodiment. Indeed, both the waveform and frequency have been improved beyond what was possible for the isolated neural model. We conclude that the body and environment are likely to be important components of the subsystem that generates locomotion in the worm.

This work was funded by the EPSRC, grant EP/C011961. NC was funded by the EPSRC, grant EP/C011953. Thanks to Stefano Berri for movies of worms and behavioural data.

Appendix A: Neural Model

Neurons are assumed to have graded potentials [11–13]. In particular, motor neurons (VB and DB) and are modelled by leaky integrators with a transmembrane potential $V(t)$ following:

$$C \frac{dV}{dt} = -G(V - E_{\text{rev}}) - I^{\text{shape}} + I^{\text{AVB}}, \quad (\text{A-1})$$

where C is the cell’s membrane capacitance; E_{rev} is the cell’s effective reversal potential; and G is the total effective membrane conductance. Sensory input $I^{\text{shape}} = \sum_{j=1}^n (V - E_j^{\text{stretch}}) G_j^{\text{stretch}} \sigma_j^{\text{stretch}}(\theta_j)$ is the stretch receptor input from the shape of the body, where E_j^{stretch} is the reversal potential of the ion channels, θ_j is the bending angle of unit j and $\sigma_j^{\text{stretch}}$ is a sigmoid response function of the stretch receptors to the local bending. The stretch receptor activation function is given by $\sigma^{\text{stretch}}(\theta) = 1/[1 + \exp(-(\theta - \theta_0)/\delta\theta)]$ where the steepness parameter $\delta\theta$ and the threshold θ_0 are constants. The command input current $I^{\text{AVB}} = G^{\text{AVB}}(V_{\text{AVB}} - V)$ models gap junctional coupling with AVB (with coupling strength G^{AVB} and denoting AVB voltage by V_{AVB}). Note that in the model, AVB is assumed to have a sufficiently high capacitance, so that the gap junctional currents have a negligible effect on its membrane potential.

Segment bending in this model is given as a summation of an output function from each of the two neurons:

$$\frac{d\theta}{dt} = \sigma_{VB}^{\text{out}}(V) - \sigma_{DB}^{\text{out}}(V), \quad (\text{A-2})$$

where $\sigma^{\text{out}}(V) = \omega_{\text{max}}/[1 + \exp(-(V - V_0)/\delta V)]$ with constants ω_{max} , δV and V_0 . Note that dorsal and ventral muscles contribute to bending in opposite directions (with θ and $-\theta$ denoting ventral and dorsal bending, respectively).

Table A-1. Parameters for a self-oscillating tail unit (as in Ref. [12]).

Parameter	Value	Parameter	Value	Parameter	Value
E_{rev}	-60mV	V_{AVB}	-30.7mV	C	5pF
G_{VB}	19.07pS	G_{DB}	17.58pS	$G_{\text{VB}}^{\text{AVB}}$	35.37pS
$G_{\text{DB}}^{\text{AVB}}$	13.78pS	$G_{\text{VB}}^{\text{stretch}}$	98.55pS	$G_{\text{DB}}^{\text{stretch}}$	67.55pS
E_{stretch}	60mV	$\theta_{0,\text{VB}}$	-18.68°	$\theta_{0,\text{DB}}$	-19.46°
$\delta\theta_{\text{VB}}$	0.1373°	$\delta\theta_{\text{DB}}$	0.4186°	$\omega_{\text{max},\text{VB}}$	6987°/sec
$\omega_{\text{max},\text{DB}}$	9951°/sec	$V_{0,\text{VB}}$	22.8mV	$V_{0,\text{DB}}$	25.0mV
δV_{VB}	0.2888mV/sec	δV_{DB}	0.0826mV/sec		

Table A-2. Parameters for body units and tail-body interactions as in Ref. [12]. All body-unit parameters that are not included here are the same as for the tail unit.

Parameter	Value	Parameter	Value	Parameter	Value
G_{VB}	26.09pS	G_{DB}	25.76pS	$G_{\text{VB}}^{\text{stretch}'}$	16.77pS
$G_{\text{DB}}^{\text{stretch}'}$	18.24pS	$E^{\text{stretch}'}$	60mV	$\theta'_{0,\text{VB}}$	-19.14°
$\theta'_{0,\text{DB}}$	-13.26°	$\delta\theta'_{\text{VB}}$	1.589°/sec	$\delta\theta'_{\text{DB}}$	1.413°/sec

Appendix B: Physical Model

The physical model consists of N rigid beams which form the boundaries between the $N - 1$ units. The i^{th} beam can be described in one of two ways: either by the (x, y) coordinates of the centre of mass (CoM_i in Fig. 1) and angle ϕ_i , or by the (x, y) coordinates of its two end points (\mathbf{P}_i^D and \mathbf{P}_i^V in Fig. 1). Each formulation has its own advantages and is used where appropriate.

B.1 Spring Forces

The rigid beams are connected to each of their neighbours by two horizontal (h) springs and two diagonal (d) springs, directed along the vectors

$$\begin{aligned} \Delta_{k,i}^h &= \mathbf{P}_{i+1}^k - \mathbf{P}_i^k \text{ for } k = D, V \\ \Delta_{m,i}^d &= \mathbf{P}_{i+1}^k - \mathbf{P}_i^l \text{ for } k = D, V, l = V, D \text{ and } m = 1, 2, \end{aligned} \quad (\text{B-1})$$

for $i = 1 : N - 1$, where $\mathbf{P}_i^k = (x_i^k, y_i^k)$ are the coordinates of the ends of the i^{th} beam. The spring forces $F_{(s)}$ depend on the length of these vectors, $\Delta_{k,i}^j = |\Delta_{k,i}^j|$

and are collinear to them. The magnitude of the horizontal and diagonal spring forces are piecewise linear functions

$$F_{(s)}^h(\Delta) = \begin{cases} \kappa_{S2}^h(\Delta - L_2^h) + \kappa_{S1}^h(L_2^h - L_0^h) & : \Delta > L_2^h \\ \kappa_{S1}^h(\Delta - L_0^h) & : L_2^h > \Delta > L_0^h \\ \kappa_{C2}^h(\Delta - L_1^h) + \kappa_{C1}^h(L_1^h - L_0^h) & : \Delta < L_1^h \\ \kappa_{C1}^h(\Delta - L_0^h) & : \text{otherwise} \end{cases}, \quad (\text{B-2})$$

$$F_{(s)}^d(\Delta) = \begin{cases} \kappa_{C2}^d(\Delta - L_1^d) + \kappa_{C1}^d(L_1^d - L_0^d) & : \Delta < L_1^d \\ \kappa_{C1}^d(\Delta - L_0^d) & : L_1^d < \Delta < L_0^d \\ 0 & : \text{otherwise} \end{cases}, \quad (\text{B-3})$$

where spring (κ) and length (L) constants are given in Table B-1.

Table B-1. Parameters of the physical model. Note that values for θ_0 and θ'_0 differ from Ref. [12] and Table A-1.

Parameter	Value	Parameter	Value	Parameter	Value
D	$80\mu\text{m}$	L_0^h	$50\mu\text{m}$	L_1^h	$0.5L_0^h$
L_2^h	$1.5L_1^h$	L_0^d	$\sqrt{L_0^{h2} + D^2}$	L_1^d	$0.95L_0^d$
κ_{S1}^h	$20\mu\text{N}\cdot\text{m}^{-1}$	κ_{S2}^h	$10\kappa_{S1}^h$	κ_{C1}^h	$0.5\kappa_{S1}^h$
κ_{C2}^h	$10\kappa_{C1}^h$	κ_{C1}^d	$50\kappa_{S1}^h$	κ_{C2}^d	$10\kappa_{C1}^d$
f_{muscle}	$0.005L_0^h\kappa_{C1}^h$	$c_{\parallel} = c_{\perp}$	$80 \times 10^{-6}\text{kg}\cdot\text{s}^{-1}$	$\theta_{0,\text{VB}}$	-29.68°
$\theta_{0,\text{DB}}$	-8.46°	$\theta'_{0,\text{VB}}$	-22.14°	$\theta'_{0,\text{DB}}$	-10.26°

B.2 Muscle Forces

Muscle forces $F_{(m)}$ are directed along the horizontal vectors $\Delta_{k,i}^h$ with magnitude

$$F_{(m)k,i} = f_{\text{muscle}}A_{k,i} \text{ for } k = D, V \text{ and } i = 1 : N - 1, \quad (\text{B-4})$$

where f_{muscle} is a constant (see Table B-1) and $A_{k,i}$ are scalar activation functions for the dorsal and ventral muscles, determined by

$$(A_{D,i}, A_{V,i}) = \begin{cases} (\theta_i(t), 0) & \text{if } \theta_i(t) \geq 0 \\ (0, -\theta_i(t)) & \text{if } \theta_i(t) < 0, \end{cases} \quad (\text{B-5})$$

where $\theta_i(t) = \int_0^t \frac{d\theta_i}{dt} dt$ is the integral over the output of the neural model.

B.3 Total Point Force

With the exception of points on the outer beams, each point i is subject to forces $\mathbf{F}_{D,i}$ and $\mathbf{F}_{V,i}$, given by differences of the spring and muscle forces from the corresponding units (i and $i - 1$):

$$\begin{aligned} \mathbf{F}_{D,i} &= (\mathbf{F}_{(s)D,i}^h - \mathbf{F}_{(s)D,i-1}^h) + (\mathbf{F}_{(s)1,i}^d - \mathbf{F}_{(s)2,i-1}^d) + (\mathbf{F}_{(m)D,i} - \mathbf{F}_{(m)D,i-1}) \\ \mathbf{F}_{V,i} &= (\mathbf{F}_{(s)V,i}^h - \mathbf{F}_{(s)V,i-1}^h) + (\mathbf{F}_{(s)2,i}^d - \mathbf{F}_{(s)1,i-1}^d) + (\mathbf{F}_{(m)V,i} - \mathbf{F}_{(m)V,i-1}). \end{aligned} \quad (\text{B-6})$$

Since the first beam has no anterior body parts, and the last beam has no posterior body parts, all terms with $i = 0$ or $i = N$ are taken as zero.

B.4 Equations of Motion

Motion of the beams is calculated from the total force acting on each of the $2N$ points. Since the points \mathbf{P}_i^D and \mathbf{P}_i^V are connected by a rigid beam, it is convenient to convert $\mathbf{F}_{(t)\mathbf{k},i}$ to a force and a torque acting on the beam's centre of mass.

Rotation by ϕ_i converts the coordinate system of $\mathbf{F}_{(t)\mathbf{k},i} = (F_{(t)\mathbf{k},i}^x, F_{(t)\mathbf{k},i}^y)$ to a new system $\mathbf{F}'_{(t)\mathbf{k},i} = (F_{(t)\mathbf{k},i}^\perp, F_{(t)\mathbf{k},i}^\parallel)$ with axes perpendicular to (\perp) and parallel with (\parallel) the beam:

$$\begin{aligned} F_{(t)\mathbf{k},i}^\perp &= F_{(t)\mathbf{k},i}^x \cos(\phi_i) + F_{(t)\mathbf{k},i}^y \sin(\phi_i) \\ F_{(t)\mathbf{k},i}^\parallel &= F_{(t)\mathbf{k},i}^y \cos(\phi_i) - F_{(t)\mathbf{k},i}^x \sin(\phi_i). \end{aligned} \quad (\text{B-7})$$

The parallel components are summed and applied to CoM_{*i*}, resulting in pure translation. The perpendicular components are separated into odd and even parts (giving rise to a torque and force respectively) by

$$\begin{aligned} F_i^{\perp,\text{even}} &= \frac{(F_{(t)D,i}^\perp + F_{(t)V,i}^\perp)}{2} \\ F_i^{\perp,\text{odd}} &= \frac{(F_{(t)D,i}^\perp - F_{(t)V,i}^\perp)}{2}. \end{aligned} \quad (\text{B-8})$$

As in Ref. [8] we disregard inertia, but include Stokes' drag. Also following Ref. [8], we allow for different constants for drag in the parallel and perpendicular directions, given by c_\parallel and c_\perp respectively. The motion of CoM_{*i*} is therefore

$$\begin{aligned} V_{(\text{CoM}),i}^\parallel &= \frac{1}{c_\parallel} (F_{(t)D,i}^\parallel + F_{(t)V,i}^\parallel) \\ V_{(\text{CoM}),i}^\perp &= \frac{1}{c_\perp} (2F_i^{\perp,\text{even}}) \\ \omega_{(\text{CoM}),i} &= \frac{1}{rc_\perp} (2F_i^{\perp,\text{odd}}), \end{aligned} \quad (\text{B-9})$$

where $r = 0.5D$ is the radius of the worm. Finally we convert $V_{(\text{CoM}),i}^\parallel$ and $V_{(\text{CoM}),i}^\perp$ back to (x, y) coordinates with

$$\begin{aligned} V_{(\text{CoM}),i}^x &= V_{(\text{CoM}),i}^\parallel \cos(\phi_i) - V_{(\text{CoM}),i}^\perp \sin(\phi_i) \\ V_{(\text{CoM}),i}^y &= V_{(\text{CoM}),i}^\perp \cos(\phi_i) + V_{(\text{CoM}),i}^\parallel \sin(\phi_i). \end{aligned} \quad (\text{B-10})$$

Appendix C: Integrating the neural and physical model

In the neural model, the output $d\theta_i(t)/dt$ specifies the bending angles $\theta_i(t)$ for each unit. In the integrated model, $\theta_i(t)$ are taken as the input to the muscles.

Muscle outputs (or contraction) are given by unit lengths. The bending angle α_i is then estimated from the dorsal and ventral unit lengths by

$$\alpha_i = 36.2 \frac{|\Delta_{D,i}^h| - |\Delta_{V,i}^h|}{L_0^h}, \quad (\text{C-1})$$

where L_0^h is the resting unit length. (For simplicity, we have denoted the bending angles of both the neural and integrated models by θ in the Figures.)

References

1. *C. elegans* Sequencing Consortium: Genome sequence of the nematode *C. elegans*: A platform for investigating biology. *Science* **282** (1998) 2012–2018
2. White, J.G., Southgate, E., Thomson, J.N., Brenner, S.: The structure of the nervous system of the nematode *Caenorhabditis elegans*. *Philosophical Transactions of the Royal Society of London, Series B* **314** (1986) 1–340
3. Ferrée, T.C., Marcotte, B.A., Lockery, S.R.: Neural network models of chemotaxis in the nematode *Caenorhabditis elegans*. *Advances in Neural Information Processing Systems* **9** (1997) 55–61
4. Ferrée, T.C., Lockery, S.R.: Chemotaxis control by linear recurrent networks. *Journal of Computational Neuroscience: Trends in Research* (1998) 373–377
5. Wicks, S.R., Roehrig, C.J., Rankin, C.H.: A Dynamic Network Simulation of the Nematode Tap Withdrawal Circuit: Predictions Concerning Synaptic Function Using Behavioral Criteria. *Journal of Neuroscience* **16** (1996) 4017–4031
6. Tsalik, E.L., Hobert, O.: Functional mapping of neurons that control locomotory behavior in *Caenorhabditis elegans*. *Journal of Neurobiology* **56** (2003) 178–197
7. Sakata, K., Shingai, R.: Neural network model to generate head swing in locomotion of *Caenorhabditis elegans*. *Network: Computation in Neural Systems* **15** (2004) 199–216
8. Niebur, E., Erdős, P.: Theory of the locomotion of nematodes. *Biophysical Journal* **60** (1991) 1132–1146
9. Niebur, E., Erdős, P.: Theory of the Locomotion of Nematodes: Control of the Somatic Motor Neurons by Interneurons. *Mathematical Biosciences* **118** (1993) 51–82
10. Niebur, E., Erdős, P.: Modeling Locomotion and Its Neural Control in Nematodes. *Comments on Theoretical Biology* **3(2)** (1993) 109–139
11. Bryden, J.A., Cohen, N.: A simulation model of the locomotion controllers for the nematode *Caenorhabditis elegans*. In Schaal, S., Ijspeert, A.J., Billard, A., Vijayakumar, S., Hallam, J., Meyer, J.A., eds.: *Proceedings of the eighth international conference on the simulation of adaptive behavior*, MIT Press / Bradford Books (2004) 183–192
12. Bryden, J.A., Cohen, N.: Neural control of *C. elegans* forward locomotion: The role of sensory feedback. Submitted (2007)
13. Bryden, J.A.: A simulation model of the locomotion controllers for the nematode *Caenorhabditis elegans*. Master’s thesis, University of Leeds (2003)
14. Chen, B.L., Hall, D.H., Chklovskii, D.B.: Wiring optimization can relate neuronal structure and function. *Proceedings of the National Academy of Sciences USA* **103** (2006) 4723–4728